Volumetric Graphics Using Laser-Induced Microbubbles in Glycerin Containing Gold Nanorods

<u>Taisei Chiba</u>, Kota Kumagai, Yoshio Hayasaki

Center for Optical Research and Education (CORE), Utsunomiya University
7-1-2 Yoto, Utsunomiya 321-8585, Japan
Keywords: Volumetric display, Microbubble, Gold nanoparticle

ABSTRACT

A laser-induced bubble display with glycerin containing gold nanorods as a screen material was developed. The gold nanorods is used to reduce the required energy of laser pulses for the bubble formation toward a large volumetric bubble graphics.

1   INTRODUCTION

The development of technology to project 3D images such as science fiction movies is a display researcher's dream. In recent display research, volumetric displays that generate 3D pixels called voxels in real space and visualize 3D images by light emission or scattering of voxels are attracting attention. Volumetric displays are characterized by the fact that the observer does not need to wear special devices such as glasses, has no physiological discomfort, and has a wide viewing angle. Among various implementation examples, a volumetric bubble display was developed using microbubbles generated by focused irradiation of femtosecond laser pulses in liquid [1]. The principle is the generation of microbubbles originating from multi-photon excitation of liquid by high photon density at the focal point by condensing and irradiating ultrashort pulse laser into the liquid [2-9]. This phenomenon is a transition of the liquid to the gas phase that occurs when the liquid is pushed away due to a sudden rise in pressure and relaxation at the focal point. Bubbles are generated at arbitrary positions in the liquid by rapidly scanning the points in three dimensions. Since this method does not require electrical wiring between the light source and the video space, unnecessary occlusion does not occur. At this time, by using glycerin, which is a highly viscous liquid, the speed of the microbubbles rising to Stokes' equation [10] was reduced to about 1/1000 of water, enabling stereoscopic image rendering. The authors also mention colorization by illumination light, control of pixel shape by computer generated hologram, and video rewriting. However, the biggest problem with this method is to enlarge the current video size of about 1cm × 1cm × 1cm.

The image size of a volumetric bubble display needs to expand the scanning range with a lens with a long focal length, but the excitation threshold energy decreases due to the increase of the condensing diameter. Also, it is necessary to increase the repetition frequency of femtosecond lasers and increase the scanning speed of galvano scanners.

In this study, we focused on gold nanoparticle (GNP) to reduce the threshold energy for bubble generation. GNP has an optical property called localized surface plasmon resonance in which incident light and free electron vibration of particles resonate [11-15]. Localized surface plasmon resonance brings about a remarkable electric field enhancement effect of incident light. It also has an antenna effect that collects light in the very vicinity of the particles, enabling highly efficient use of light energy. GNP has a very low quantum yield due to light emission, so it can efficiently absorb absorbed light energy. It induces photothermal effects that convert it into heat. Because of its unique optical properties, GNP is a biosensor [16], optical nanofabrication [17], nanotherapy [18] and plasmon solar cells [19]. Research has been conducted in a wide range of fields. The gold nanorod (GNR), which is a rod-shaped particle, can adjust the resonance wavelength according to the aspect ratio of the particle. Using GNR, the resonance wavelength of localized surface plasmon resonance can be red-shifted to the near infrared region.

In this study, we propose a new screen material in which gold nanomaterials are dispersed in glycerin to reduce an excitation energy for bubble formation. The energy reduction offers to enlarge the display and the increase the number of pixels, in addition, no need for an amplified laser, leading to a drastical miniaturization and cost reduction of the volumetric display system. Now we try to expand a palm size system, typically $10 \times 10 \times 10 cm^3$ from the present volume image which was the size of a fingertip with less than $1 \times 1 \times 1 cm^3$.

2   EXPERIMENTS

Figure 1 shows a volumetric bubble display system. This system was composed of an amplified Ti:Sa femtosecond laser system (Micra and Legend Elite Duo, Coherent), a three-dimensional (3D) beam scanner, liquid-crystal-on-silicon spatial light modulator (LCOS-SLM; X10468-02, Hamamatsu), a mechanical shutter (Laser Shutter; LS055, NM Laser Products) , a halogen lamp (PHL-150, MEJIRO PRECISION), a CMOS image sensor (DMK 42BUC03, IMAGINGSOURCE), and a

glass cell containing a liquid screen material. A beam emitted from the femtosecond laser with a center wavelength of 800 nm and a repetition frequency of 1 kHz was adjusted the energy with a neutral density filter. Then, the phase of the beam was spatially modulated by LCOS-SLM. The focusing position was controlled by the 3D beam scanner consisting of a 2D galvano scanner (GM-1010, Canon) and an mechanical stage (ANT95-XY, AEROTECH).

The screen material was placed in glass cells each having a size of 10mm × 10mm × 45mm. The screen materials were glycerin containing pure glycerin, GNP with a diameter of 20nm, 40nm, or 80nm, GNR with a diameter of 10nm and a length of 45nm.

Microbubble generations were generated by a single laser pulse and observed with a halogen lamp, a 6X microscope, and a CMOS image sensor. The single pulse was extracted by a mechanical shutter (Laser Shutter; LS055, NM Laser Products). The bubble image was visualized through light scattering on a bubble for halogen lamp illumination.
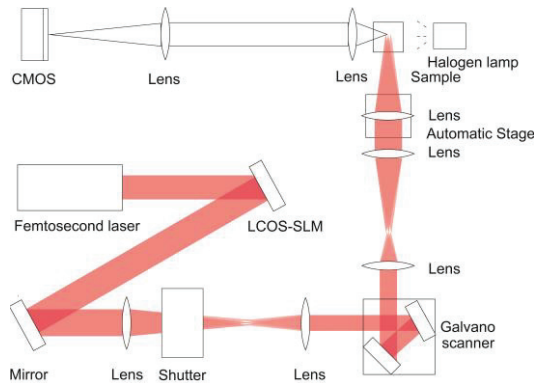
Fig. 1. Volumetric bubble display system.
The focal point of the femtosecond laser was controlled to an arbitrary position by a 3D beam scanner.

3   EXPERIMENTALRESULTS

3.1 Material dependency of bubble generation threshold

Figure 2 shows the bubble generation region in the optical axis direction for the irradiation pulse energy in a liquid screen containing glycerin, GNP with diameters of 20 nm, 60 nm, and 80 nm in glycerin at the same density as GNR. The generation region is measured five times for each energy, the points indicate experimental values, and the curves indicate average values. The bubble formation threshold for glycerin was 1.34 µJ. For GNP-containing glycerin, when the GNP particle size is 20 nm, 60 nm, and 80 nm, the bubble generation threshold drops to 1.126 µJ, 0.621 µJ, and 0.617 µJ, respectively. The bubble formation threshold of glycerin containing GNR was 0.529µJ, a decrease rate of 61%. This result is due to the resonance

wavelength of localized surface plasmon resonance depending on the particle shape.
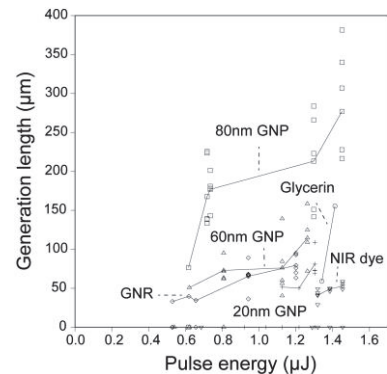
Fig. 2. Length of the bubble generation versus pulse energy.
The bubble generation area when glycerin contained GNP had different size was shown.

3.2 Threshold and generation probability versus concentration of GNR

Next, we observe the formation of bubbles in the GNR containing glycerin that showed the lowest threshold drop when the concentration was changed. Figure 3 shows the relationship between the bubble generation probability and the generation threshold for the GNR concentration. The solid line in the graph indicates the bubble generation threshold, and the broken line indicates the bubble generation probability. As the concentration increases, the generation probability increases, but the threshold does not change. From these results, it can be seen that the probability of bubble generation changes with the number of particles in the focused spot.
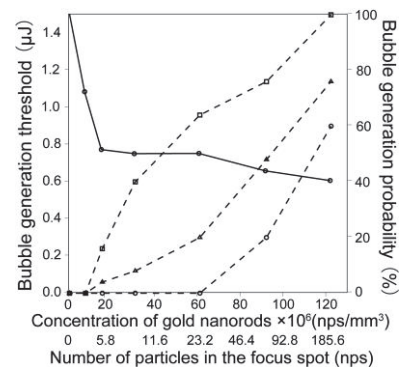
Fig. 3 Bubble generation threshold and generation probability for concentration of GNR.
the relationship between the bubble generation probability and the generation threshold for the GNR concentration was shown.

3.3 Bubble graphics in glycerin containing GNR

Figure 4 (a) was drawn in glycerin, and Fig. 4 (b) was drawn in gold nanorod-containing glycerin by scanning laser-induced microbubbles generated using a galvano scanner.   This is a video of how long is the exposure

time 5 s. Even with glycerin containing GNR, it was possible to draw images, and clearer images were obtained than those drawn in glycerin. This result is due to the number of bubbles generated with the same energy.

40.2 [μJ]   50.6 [μJ]   60.8 [μJ]   80.0 [μJ]
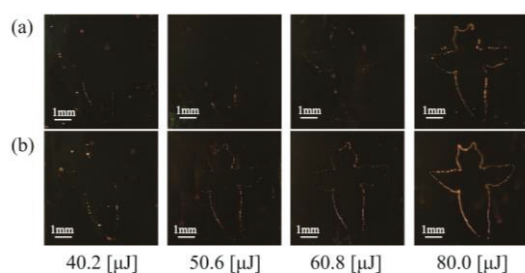
Fig. 4 Drawn graphics in (a) glycerin, (b) glycerin containing GNR.
(a) was drawn in glycerin, and (b) was drawn by in GNR-containing glycerin scanning using a galvano scanner.

4   CONCLUSIONS

We proposed a new screen for bubble displays containing GNR. This enables bubble generation with low energy and leads to the expansion of the bubble display image. We believe that elucidating the dynamics of bubble generation near GNR during liquid excitation leads to the determination of the best particle conditions for threshold energy reduction.

REFERENCES

[1] K. Kumagai, S. Hasegawa, and Y. Hayasaki, "Volumetric bubble display," Optica 4, 298-302 (2017).

[2] C. B. Schaffer, N. Nishimura, E. N. Glezer, A. M.-T. Kim, and E. Mazur, "Dynamics of femtosecond laser-induced breakdown in water from femtoseconds to microseconds," Opt. Exp. 10, 196–203 (2002).

[3] A. Vogel, J. Noack, K. Nahen, D. Theisen, S. Busch, U. Parlitz, D. X. Hammer, G. D. Noojin, B. A. Rockwell, and R. Birngruber, "Energy balance of optical breakdown in water at nanosecond to femtosecond time scales, " Appl. Phys. B 68, 271-280 (1999).

[4] E. Abraham, K. Minoshima, and H. Matsumoto, "Femtosecond laser-induced breakdown in water: time-resolved shadow imaging and two-color interferometric imaging," Optics Commun. 176, 441-452 (2000).

[5] A. Takita and Y. Hayasaki, "Interference measurement of superposition of laser-induced shock waves in water," Jpn. J. Appl. Phys. 48, 09LD04 (2009).

[6] P. Qi, Q. Su, L. Lin, and W. Liu, "Bubble dynamics driven by a few successive femtosecond laser pulses in methanol under 1 kHz," J. Opt. Soc. Am. B 35, 2727-2733 (2018).

[7] C.-D. Ohl, T. Kurz, R. Geisler, O. Lindau, W. Lauterborn, "Bubble dynamics, shock waves and sonoluminescence," Philo. Trans. A **357**, 269-294 (1999).

[8] J. Noack, D. X. Hammer, G. D. Noojin, B. A. Rockwell, A. Vogel, "Influence of pulse duration on mechanical effects after laser-induced breakdown in water," J. Appl. Phys. 83, 7488 (1998).

[9] R. Evans, S. Camacho-López, F. G. Pérez-Gutiérrez and G. Aguilar, "Pump-probe imaging of nanosecond laser-induced bubbles in agar gel", Opt. Exp. 16, 7481-7492 (2008).

[10] S. J. Lee and S. Kim, "Simultaneous measurement of size and velocity of microbubbles moving in an opaque tube using an X-ray particle tracking velocimetry technique," Experiments in Fluids 39, 492-497 (2005).

[11] S. Hashimotoa, D. Wernera, T. Uwad, "Studies on the interaction of pulsed lasers with plasmonic gold nanoparticles toward light manipulation, heat management, and nanofabrication," Journal of Photochemistry and Photobiology C: Photochemistry Reviews 13, 28– 54 (2012).

[12] M.-C. Daniel and D. Astruc, "Gold nanoparticles: assembly, supramolecular chemistry, quantum-size-related properties, and applications toward biology, catalysis, and nanotechnology," Chem. Rev. 104, 293-346 (2004).

[13] V. K. Pustovalov, A. S. Smetannikov, and V. P. Zharov, "Photothermal and accompanied phenomena of selective nanophotothermolysis with gold nanoparticles and laser pulses", Laser Phys. Lett. 1, 775-792 (2008).

[14] P. M. R. Paulo, A. Gaiduk, F. Kulzer, S. F. Gabby Krens, H. P. Spaink, T. Schmidt, and M. Orrit, "Photothermal correlation spectroscopy of gold nanoparticles in solution", J. Phys. Chem. C 113, 11451–11457 (2009).

[15] M. Kitz, S. Preisser, A. Wetterwald, M. Jaeger, G. N. Thalmann, and M. Frenz, "Vapor bubble generation around gold nano-particles and its application to damaging of cells," Bio. Opt. Exp., 2, 291-304 (2011).

[16] K. A. Willets and R. P. Van Duyne, "Localized surface plasmon resonance spectroscopy and sensing", Ann. Rev. Phys. Chem. 58, 267-297 (2007).

[17] K. Yamada, T. Itoh, and Y. Tsuboi, "Nanohole processing of polymer films based on the laser-induced superheating of Au nanoparticles", Appl. Phys. Express 1, 087001.1-087001.3 (2008).

[18] E. C. Dreaden, A. M. Alkilany, X. Huang, C. J. Murphy, and M. A. El-Sayed, "The golden age: gold nanoparticles for biomedicine," Chem. Soc. Rev. 41, 2740-2779 (2012).

[19] K. R. Catchpole, and A. Polman, "Plasmonic solar cells", Opt. Express 16, 793-800 (2010).